The Plant Cell, Vol. 20: 3080–3093, November 2008, www.plantcell.org

Cellulose Binding Protein from the Parasitic Nematode *Heterodera schachtii* Interacts with *Arabidopsis* Pectin Methylesterase: Cooperative Cell Wall Modification during Parasitism [W]

Tarek Hewezi,[a] Peter Howe,[a] Tom R. Maier,[a] Richard S. Hussey,[b] Melissa Goellner Mitchum,[c] Eric L. Davis,[d] and Thomas J. Baum[a,1]

[a] Department of Plant Pathology, Iowa State University, Ames, Iowa 50011
[b] Department of Plant Pathology, University of Georgia, Athens, Georgia 30602
[c] Division of Plant Sciences and Bond Life Sciences Center, University of Missouri, Columbia, Missouri 65211
[d] Department of Plant Pathology, North Carolina State University, Raleigh, North Carolina 27695

Plant–parasitic cyst nematodes secrete a complex of cell wall–digesting enzymes, which aid in root penetration and migration. The soybean cyst nematode *Heterodera glycines* also produces a cellulose binding protein (Hg CBP) secretory protein. To determine the function of CBP, an orthologous cDNA clone (Hs CBP) was isolated from the sugar beet cyst nematode *Heterodera schachtii*, which is able to infect *Arabidopsis thaliana*. CBP is expressed only in the early phases of feeding cell formation and not during the migratory phase. Transgenic *Arabidopsis* expressing Hs *CBP* developed longer roots and exhibited enhanced susceptibility to *H. schachtii*. A yeast two-hybrid screen identified *Arabidopsis* pectin methylesterase protein 3 (PME3) as strongly and specifically interacting with Hs CBP. Transgenic plants overexpressing *PME3* also produced longer roots and exhibited increased susceptibility to *H. schachtii*, while a *pme3* knockout mutant showed opposite phenotypes. Moreover, CBP overexpression increases PME3 activity in planta. Localization studies support the mode of action of PME3 as a cell wall–modifying enzyme. Expression of CBP in the *pme3* knockout mutant revealed that PME3 is required but not the sole mechanism for CBP overexpression phenotype. These data indicate that CBP directly interacts with PME3 thereby activating and potentially targeting this enzyme to aid cyst nematode parasitism.

INTRODUCTION

Cyst nematodes, *Heterodera* and *Globodera* spp, are sedentary parasites of plant roots in many economically important cropping systems where they cause severe yield loss (Barker and Koenning, 1998; Wrather et al., 2001). The soybean cyst nematode, *Heterodera glycines*, is regarded as the most serious pathogen problem in soybean production worldwide, and the sugar beet cyst nematode (*Heterodera schachtii*) also is a devastating pathogen to many plant species in addition to sugar beets. To sustain their subsequent sedentary parasitic stages, cyst nematodes induce the formation of elaborate feeding sites, termed syncytia, whose etiology includes substantial cell wall reorganization and dissolution in addition to dramatic cytoplasmic and nuclear changes (Williamson and Hussey, 1996). The parasitic feats of cyst nematodes during penetration, migration, syncytium formation and maintenance, and feeding are aided by proteinaceous stylet secretions, which are the expression products of specific parasitism genes in nematode esophageal gland cells (Davis et al., 2004, 2008). Parasitism proteins are synthesized as preproteins with N-terminal signal peptides targeting them to the gland cell endoplasmic reticulum and the secretory pathway (Qin et al., 2000; Wang et al., 2001). Nematode parasitism proteins are developmentally produced and released through the stylet into plant tissues and cells to promote the parasitic interaction. While two subventral gland cells are most active during the early stages of parasitism (i.e., root penetration and migration) and early events of syncytium formation, the single dorsal gland cell becomes most active in the later stages of syncytium formation, maintenance, as well as during feeding.

A large number of *H. glycines* parasitism genes were identified by different approaches, most recently the microaspiration of esophageal gland cell cytoplasm followed by the construction and mining of gland cell cDNA libraries (Gao et al., 2001, 2003; Wang et al., 2001; de Boer et al., 2002). Among the subventral gland-produced parasitism proteins of *H. glycines* was a short protein with high similarity to the cellulose binding domain (CBD) of previously identified *H. glycines* endoglucanases (Smant et al., 1998). Additionally, actual binding to cellulose was documented experimentally; therefore, this protein was termed cellulose binding protein, or Hg CBP (Gao et al., 2004). Cyst nematode endoglucanases produced in the subventral glands and secreted during the migratory phase are thought to be key parasitic tools to breach root cell walls (Smant et al., 1998; de Boer et al.,

[1] Address correspondence to tbaum@iastate.edu.
The author responsible for distribution of materials integral to the findings presented in this article in accordance with the policy described in the Instructions for Authors (www.plantcell.org) is: Thomas J. Baum (tbaum@iastate.edu).
[W] Online version contains Web-only data.
www.plantcell.org/cgi/doi/10.1105/tpc.108.063065

1999; Wang et al., 1999; Goellner et al., 2001). Cyst nematode endoglucanase expression sharply decreases as syncytia are initiated (de Boer et al., 1999; Goellner et al., 2000); subsequently, plant endoglucanase expression is upregulated within the developing feeding cells (Goellner et al., 2001).

The plant cell wall provides essential mechanical strength and rigidity and also acts as a physical barrier against pathogens. The primary cell wall is a network of crystalline cellulose microfibrils embedded in a matrix of hemicelluloses and pectins. Cellulose is a particularly difficult polymer to degrade, as it is insoluble and is present as hydrogen-bonded crystalline fibers (Doi and Kosugi, 2004). Microorganisms have evolved the ability to break down plant cell walls, which involves the production and secretion of a large number of cellulase enzymes that can act synergistically (Collmer and Keen, 1986). In the case of aerobic fungi and bacteria, the majority of these cellulases have a specific modular structure consisting of a catalytic domain, responsible for hydrolysis, and a CBD responsible for attachment of the enzymes to the insoluble cellulose substrate.

CBD-containing proteins that have no apparent hydrolytic activity but exhibit cellulose binding activity were first isolated from the cellulolytic bacterium *Clostridium cellulovorans* (Shoseyov and Doi, 1990). This CBP exhibited a relatively high affinity for cellulose and was found to be essential for the degradation of crystalline cellulose (Goldstein et al., 1993). It is thought that CBD determines the efficiency of degradation of insoluble cellulose by concentrating cellulase catalytic domains on the surface of the insoluble cellulose substrate (Tomme et al., 1998; Carrard et al., 2000).

More than 200 CBDs, either as CBPs alone or as part of catalytic proteins, have been identified from different organisms and classified into different families according to their amino acid sequence similarities in the CAZY database (http://afmb.cnrs-mrs.fr/~pedro/CAZY/cbm.html). CBDs also differ in their binding affinity and substrate specificity (Carrard et al., 2000; McCartney et al., 2006). In plant-parasitic nematodes, the first CBP gene to be identified was Mi *CBP-1* from the root-knot nematode *Meloidogyne incognita* (Ding et al., 1998). Mi *CBP-1* encodes a signal peptide, a C-terminal CBD, and a 71–amino acid N-terminal region with unknown function. These latter two domains are joined by a linker peptide. Mi CBP-1 was found to bind to cellulose and plant cell walls but lacked cellulase activity. Strong evidence for secretion and involvement of Mi CBP-1 in pathogenesis was provided by the detection of this protein in stylet secretions. Hg *CBP* from *H. glycines* was the second such cDNA from a nematode (Gao et al., 2003, 2004) and the first CBP identified in nematodes consisting only of a signal peptide and a CBD. Like Mi CBP-1, recombinant Hg CBP protein had no hydrolytic activity on carboxymethyl-cellulose but was able to bind to cellulose in an in vitro assay. Similarly, the potato cyst nematode (*Globodera rostochiensis*) secrets a noncellulase CBD-containing protein. However, another region of this protein was similar to plant expansins, and cell wall–softening activity could be shown experimentally (Qin et al., 2004). Hg CBP does not have similarity to expansins, and its functional roles in plant–nematode interactions still remain elusive. However, the developmental expression patterns of Hg *CBP* during different nematode life stages suggest a role in pathogenesis most likely during the establishment and maintenance of the nematode feeding sites (Gao et al., 2004).

Very limited data regarding the effects of CBPs on the living plant cell are available. It has been shown that a recombinant bacterial CBD enhanced elongation of different plant cells in vitro (Shpigel et al., 1998). Similarly, a bacterial CBD from *C. cellulovorans* was also found to modulate plant growth in transgenic poplar plants leading to a significant increase in biomass production in selected clones when compared with the wild type (Shoseyov et al., 2001). Although these data indicate that CBDs can modulate plant growth, the mechanisms by which these unique CBDs affect plant development or susceptibility to plant-parasitic nematodes still remain obscure. In this study, we used an integrative approach to investigate the function of CBP during cyst nematode parasitism. Interestingly, we discovered an unexpected mode of action of cyst nematode CBPs that entails a direct interaction with a plant endogenous pectin methyl esterase protein.

RESULTS

Identification of the Sugar Beet Cyst Nematode *CBP-1* cDNA

To make use of the extensive resources and technical advantages offered by the model plant *Arabidopsis thaliana*, which is a host to the sugar beet cyst nematode *H. schachtii* (Sijmons et al., 1991), we isolated the *H. schachtii* homolog of *H. glycines* CBP using a homology-based PCR approach. Identical to the Hg CBP (Gao et al., 2004), the *H. schachtii CBP* cDNA (Hs *CBP*) contained an open reading frame of 396 bases encoding a 132–amino acid protein with an N-terminal signal peptide for secretion and a CBD of 107 amino acids. The *H. schachtii* protein had 94% identity and 97% similarity to the CBP of *H. glycines* (see Supplemental Figure 1 online).

Localization of *CBP* Transcripts

One of the hallmark characteristics of parasitism genes is their exclusive expression in the secretory esophageal gland cells. To provide evidence that *CBP* is expressed uniquely in the esophageal gland cells, the tissue localization of *CBP* mRNA was analyzed in different parasitic life stages of *H. schachtii* using in situ mRNA hybridization. The digoxigenin-labeled antisense cDNA probes of *CBP* hybridized exclusively with transcripts accumulating within the subventral esophageal gland cells (see Supplemental Figure 2A online). No signal was detected when the control sense cDNA probes were used. The Hg *CBP* was also shown to hybridize exclusively to the subventral esophageal gland cells in *H. glycines* (Gao et al., 2003).

Developmental Expression Pattern of CBP

The expression profile of a given parasitism gene will identify the most likely time of activity of the corresponding parasitism protein. Therefore, we assessed the *CBP* expression profile using real-time RT-PCR through the six *H. schachtii* developmental stages of eggs, preparasitic second-stage juvenile (pre-J2),

parasitic J2 (par-J2), third-stage juvenile (J3), fourth-stage juvenile (J4), and adult females. *CBP* mRNA steadily increased from eggs to J3 and then rapidly declined after the J3 stage (see Supplemental Figure 2B online). This expression pattern is very similar to that previously observed in *H. glycines* (Gao et al., 2004; Elling et al., 2007a) and supports a role in pathogenicity as a secreted protein. The expression peak at the J3 stage again suggests a role during the early phases of syncytium formation.

Transgenic *Arabidopsis* Plants Expressing *CBP* Are Altered in Morphology and Susceptibility to *H. schachtii*

It has been shown that CBDs can affect plant growth and development in vitro and in planta (Shpigel et al., 1998; Shoseyov et al., 2001). Therefore, it was particularly interesting to see if *CBP* overexpression produces similar phenotypes. In addition, if CBP has a function in cell wall modification, one can reasonably postulate that ectopic expression in *Arabidopsis* should alter cell wall–associated phenotypes. To investigate this, we transformed *Arabidopsis* with gene constructs containing the 35S cauliflower mosaic virus (CaMV) promoter driving the Hs *CBP* cDNA either with the native signal peptide ($^{SP+}$CBP) or without ($^{SP-}$CBP). Presence or absence of the signal peptide was thought to potentially be helpful in discerning if the site of CBP action is in the apoplast or the symplast of the host plant, respectively. For each of the two constructs, multiple independent homozygous T3 lines were identified. Lines 2-4, 21-9, and 30-6, containing *CBP* with signal peptide, and lines 12-10, 26-3, and 28-7, containing *CBP* without signal peptide, were found to express *CBP* at high levels as quantified by real-time RT-PCR and were used in further studies. Seeds from these six homozygous lines were planted on nutrient medium, and root length was measured 9 d after planting. Interestingly, expression of $^{SP+}$CBP as well as $^{SP-}$CBP produced plants with significantly increased root lengths (Figures 1A and 1B) ranging from 21.68 mm ± 0.91 mm to 33.09 mm ± 2.03 mm in the $^{SP+}$CBP transgenic lines and 26.67 mm ± 1.57 mm to 33.88 mm ± 0.82 mm in the $^{SP-}$CBP transgenic lines compared with the wild-type control (16.71 mm ± 0.97 mm), while no statistically significant differences were detected between lines with and without the signal peptide coding sequence. Also, no significant differences were observed in the aboveground parts of any CBP transgenic lines when compared with the wild type. These dramatic changes in morphology document that the nematode-produced CBP has a biological function in planta. Also, the in planta expression phenotype changes are reminiscent of those seen by others investigating bacterial CBDs in planta, suggesting a conserved mode of action of both nematode and bacterial molecules, although bacterial CBDs also influenced shoot phenotypes (Shpigel et al., 1998).

Since the signal peptide had no effect on plant phenotype, it can be postulated that, most likely, the nematode signal peptide does not properly work in planta and that the observed plant phenotypes are due to a cytoplasmic accumulation of CBP. To test this hypothesis, we fused the 3′-ends of both *$^{SP+}$CBP* and *$^{SP-}$CBP* cDNAs to the green fluorescent protein (GFP) and β-glucuronidase (GUS) reporter genes (*$^{SP+}$CBP*:GFP:GUS and *$^{SP-}$CBP*:GFP:GUS) under the control of double CaMV 35S promoters. Both constructs were delivered into onion epidermal cells by biolistic bombardment. After 24 h of incubation following bombardment, the onion epidermal cells were treated with 1 M sucrose solution to separate cytoplasm from cell walls (plasmolysis). For both constructs, GFP signals were localized only within transformed plant cells rather than in cell walls (Figure 1C), suggesting that the native nematode signal peptide in fact did not function properly in planta and that the observed CBP overexpression phenotypes are due to events that are initiated in the cytoplasm.

Secretion of CBP by cyst nematodes into host plants should facilitate parasitism. Therefore, we determined the susceptibility of the same six CBP-expressing transgenic *Arabidopsis* lines described above in nematode infection assays in which the numbers of female nematodes were determined and used to quantify plant susceptibility. Four out of the six transgenic lines expressing *CBP* cDNAs were significantly more susceptible to *H. schachtii* than the wild type (Figure 1D). The remaining two lines also showed increases in susceptibility; however, they were statistically nonsignificant. It is important to mention that there was a clear relationship between *CBP* expression level and the degree of susceptibility. The two lines that showed the lowest susceptibility among all test lines were those with the lowest *CBP* expression levels. In other words, these lines required between 1.6 and 3.57 additional PCR cycles to reach the transgene detection threshold (see Supplemental Table 1 online). These results establish that CBP can function in planta in a manner conducive to successful cyst nematode parasitism.

To evaluate whether this elevated level of susceptibility was a specific result of CBP functioning as a cyst nematode parasitism protein or merely was a function of the increased root area available for penetrating nematodes, two lines (21-9 and 26-3) showing the most significant increase in root length were inoculated with *H. schachtii* J2 along with the wild-type control, and 4 d after inoculation the total number of penetrated nematodes was counted. Data from two independent experiments revealed no statistically significant differences between the tested lines and the wild-type control (see Supplemental Figure 3 online). These data indicate that the increased susceptibility to *H. schachtii* is not due to elevated penetration rates conditioned by enlarged roots but rather is due to postpenetration effects of the *H. schachtii* CBP parasitism protein.

Similarly, all six transgenic *Arabidopsis* lines expressing *CBP* cDNAs were inoculated with the root knot nematode *M. incognita*, which uses a different penetration and in planta migration strategy and induces different feeding cells than cyst nematodes. Although slightly elevated, no statistically significant effect of CBP on plant susceptibility to *M. incognita* was observed (see Supplemental Figure 4 online), indicating that CBP functions specifically to modulate parasitic success of cyst nematodes.

To further explore why *CBP*-expressing *Arabidopsis* lines are more susceptible to *H. schachtii*, we measured the size of syncytia formed in transgenic and wild-type *Arabidopsis* lines. For this purpose, 10 single-nematode syncytia were randomly selected for size measurement from lines 21-9 and 26-3 10 d after inoculation. No statistically significant differences were observed between the size of syncytia from transgenic lines expressing *CBP* (0.249 mm^2 ± 0.01 mm^2) and the wild-type

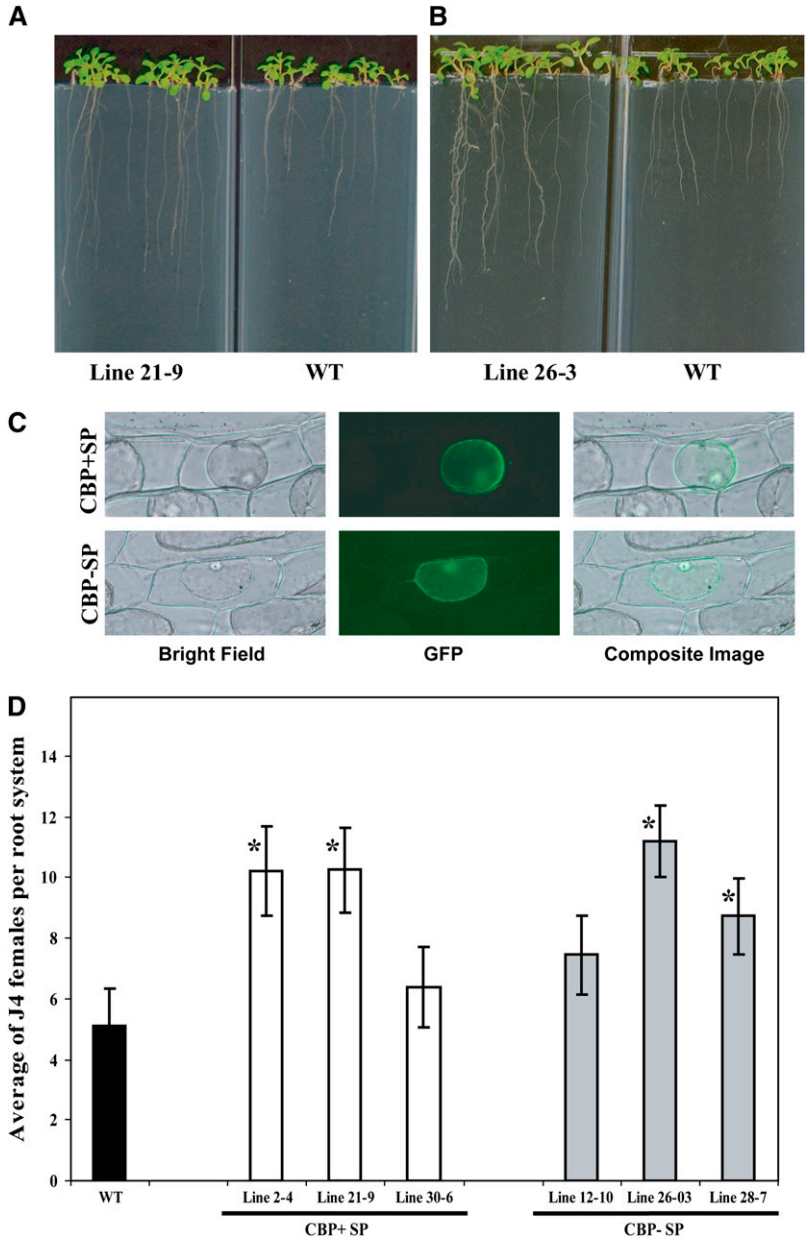

Figure 1. Characterization of Hs *CBP*.

(A) and **(B)** Expression of Hs *CBP* in *Arabidopsis* increases root length. Homozygous T3 lines expressing either Hs *CBP* with **(A)** or without **(B)** signal peptide exhibited significantly longer root systems ranging from 21.68 mm ± 0.91 mm to 33.09 mm ± 2.03 mm in the transgenic lines expressing *CBP* with signal peptide and 26.67 mm ± 1.57 mm to 33.88 mm ± 0.82 mm in the transgenic lines expressing *CBP* without signal peptide compared with wild-type C24 (16.71 mm ± 0.97 mm) at 10 d after planting as determined by unadjusted paired *t* tests ($P < 0.01$). This observation was true with all six homozygous T3 lines tested.

(C) Subcellular localization of Hs CBP. Hs *CBP* cDNA with or without signal peptide-coding sequence was fused to the GFP and GUS reporter genes and expressed in onion epidermal cells. After plasmolysis, GFP fluorescence was retained inside the protoplast in both cases.

(D) Transgenic *Arabidopsis* plants expressing Hs *CBP* showed enhanced susceptibility to *H. schachti.* Homozygous T3 lines expressing either Hs *CBP* with (lines 2-4, 21-9, and 30-6) or without (lines 12-10, 26-3, and 28-7) the native signal peptide were planted on modified Knop's medium, and 2-week-old seedlings were inoculated with ~250 surface-sterilized J2 *H. schachtii* nematodes. Two weeks after inoculation, the number of J4 female nematodes per root system was determined. Data are presented as the mean ± SE. Mean values significantly different from the wild type are denoted by an asterisk as determined by unadjusted paired *t* tests ($P < 0.05$). Identical results were obtained from at least two independent experiments.

control (0.231 $mm^2 \pm 0.018\ mm^2$). These results indicate that the mode of action responsible for increased susceptibility of *CBP*-expressing *Arabidopsis* lines does not involve an enlargement of syncytia per se.

CBP Interacts with *Arabidopsis* Pectin Methylesterase 3

Judging from the fact that CBP lacks an obvious catalytic domain, it is plausible that interactions with other proteins are required for CBP function. We therefore set out to identify host proteins that interact with CBP and used a yeast two-hybrid (Y2H) approach to screen three *Arabidopsis* Y2H prey libraries, which we generated from roots at 3, 7, and 10 d after *H. schachtii* inoculation. These libraries, consequently, contained cDNA clones from parasitic *H. schachtii* at the different time points after infection along with the cDNAs from *Arabidopsis* plants at various stages of nematode parasitism. After screening of $\sim 15.62 \times 10^6$ yeast colonies from the three prey libraries in roughly equal proportions, we identified 90 clones of candidate interactor (prey) proteins. Prey plasmids were rescued from these yeast colonies, and DNA sequencing revealed that these clones coded for nine independent *Arabidopsis* proteins. The specificity of these putative interactions was further scrutinized as described in Methods, and only one protein consistently and reproducibly gave a specific interaction with Hs CBP (see Supplemental Figure 5A online). This protein was *Arabidopsis* pectin methylesterase 3 (PME3; At3g14310). The positive interaction between Hs CBP and PME3 was further confirmed by α-Gal quantitative assays (Figure 2A). To provide additional confirmatory evidence of this interaction, bimolecular fluorescent complementation (BiFC) assays were performed. Hs CBP and PME3 without signal peptides were fused to N-terminal and C-terminal halves of yellow fluorescent protein (YFP), respectively, and coexpressed in onion epidermal cells. The interaction between CBP and PME3 reconstituted the activity of YFP in the cytoplasm of transformed cells (Figure 2B). No YFP fluorescence was obtained when the YFP fragment constructs containing *CBP* or *PME3* were bombarded alone or in combination with empty vectors or an unrelated nematode gene.

Because the *Arabidopsis* genome contains at least 66 PME-related genes, we tested whether other PME proteins can bind to CBP in Y2H assays as well. In these experiments, PME2 (At1g53830), which shares the highest sequence similarity with PME3 among all PME family members, was cloned with and without signal peptide in the prey vector. Also, PME1 (At1g53840), a nonsecretory protein, was cloned in the prey vector. The potential interactions between these two PME proteins and CBP were tested after cotransformation of prey and

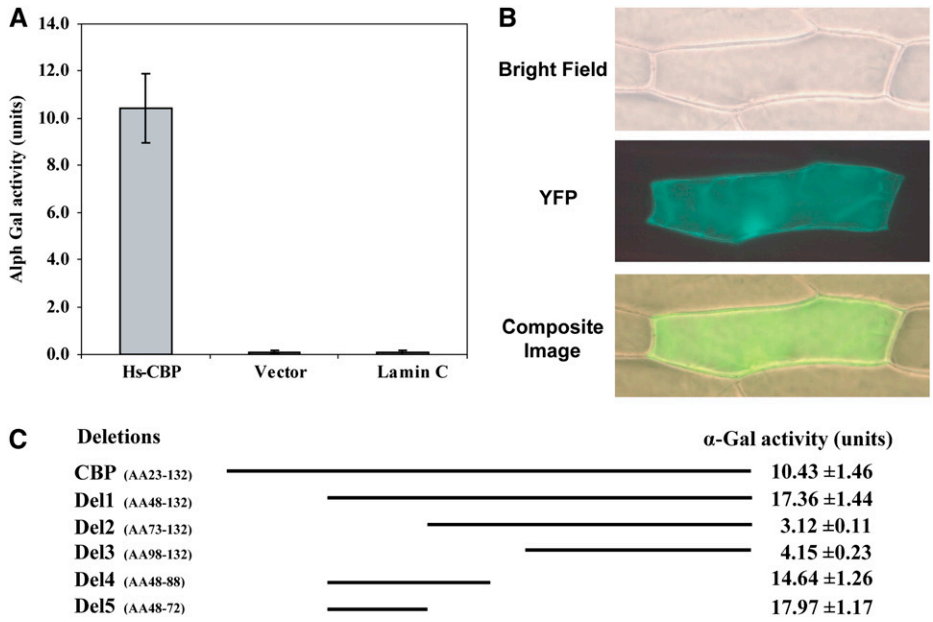

Figure 2. Hs CBP Reproducibly Interacts with PME3.

(A) α-Gal quantitative assays of the CBP/PME3 interaction. Yeast strain AH109 was cotransformed with the prey plasmid in combination with either the CBP bait vector, pGBKT7-lam (expressing lamin C as a GAL-4 DNA-BD fusion), or the empty pGBKT7 bait vector and plated on SD/-Leu/-Trp. Three days after culture, 10 separate colonies per combination were picked to quantify the interaction using α-Gal activity. Activity was seen only in yeast cells containing the PME3 prey plasmid and the CBP bait vector. The experiment was repeated four times with identical results.

(B) BiFC visualization of the CBP/PME3 interaction. Onion epidermal cells were cobombarded with constructs expressing the nEYFP-CBP and cEYFP-PME3 and bright-field, YFP and overlay of bright field, and YFP images were taken 20 h after bombardment.

(C) Mapping the CBP domain involved in the interaction with PME3. Yeast strain AH109 cotransformed with prey plasmid and the different bait constructs indicated in the scheme were streaked on SD/-Leu/-Trp, and 3 d after culture, 10 separate colonies per construct were picked to quantify α-galactosidase activity. The assays were repeated three times with identical results.

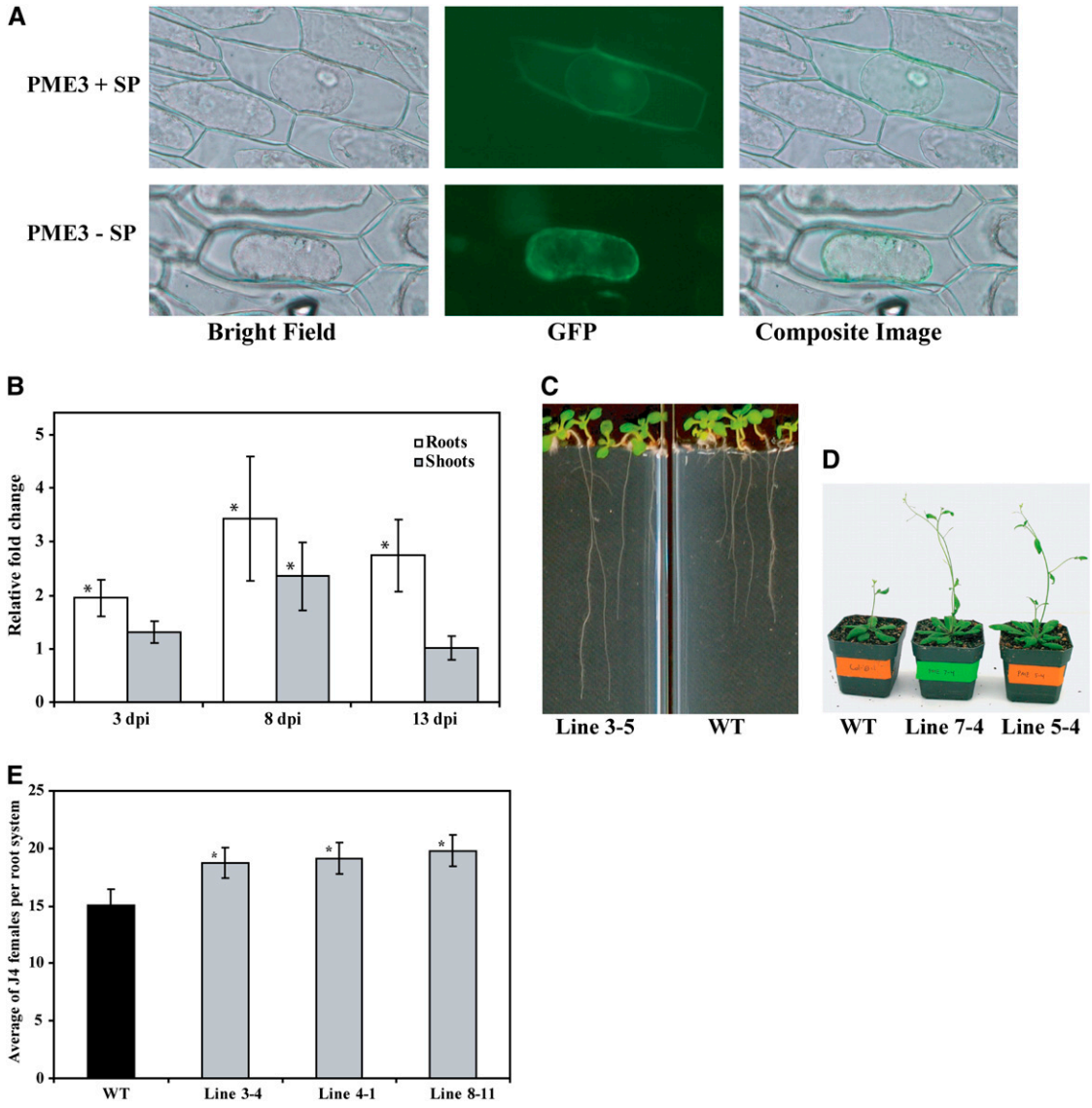

Figure 3. Characterization of *Arabidopsis PME3*.

(A) Subcellular localization of PME3. *PME3* cDNA with or without signal peptide-coding sequence was fused to GFP and GUS reporter proteins and expressed in onion epidermal cells. After plasmolysis, GFP signal was detected both in the cell wall and the cytoplasm of the transformed cells expressing whole PME3 (top panel). By contrast, in onion cells expressing PME3 without signal peptide, the GFP signal was detected only in the cytoplasm (bottom panel).

(B) Upregulation of *PME3* in response to *H. schachtii* infection. The mRNA expression level of *PME3* was measured by quantitative real-time RT-PCR in wild-type (C24) root and shoot tissues. Infected and noninfected tissues were collected at 3, 8, and 13 d after inoculation (dpi). The fold-change values were calculated using the $2^{-\Delta\Delta CT}$ method and represent changes of mRNA abundance in infected tissues relative to noninfected controls. Data are the average of three independent biological experiments, each consisting of four technical replicates. Mean values significantly different from 1.0 (no change) are indicated by an asterisk as determined by paired *t* tests ($P < 0.01$).

(C) and **(D)** Transgenic *Arabidopsis* plants overexpressing *PME3* are altered in morphology. Homozygous T3 lines overexpressing *PME3* displayed longer roots **(C)** and taller shoots **(D)** than the wild type (Col-0).

(E) Transgenic *Arabidopsis* plants overexpressing *PME3* revealed increased susceptibility to *H. schachtii.* Homozygous T3 lines overexpressing *PME3* (lines 3-4, 4-1, and 8-11) were planted on modified Knop's medium, and 2-week-old seedlings were inoculated with ~250 surface-sterilized J2 *H. schachtii* nematodes. Two weeks after inoculation, the number of J4 female nematodes per root system was determined. Data are presented as the mean ± SE. Mean values significantly different from the wild type (Col-0) as determined by unadjusted paired *t* tests ($P < 0.05$) are denoted by an asterisk. Identical results were obtained from at least two independent experiments.

bait plasmids into yeast. No interaction between CBP and these preys was detected, indicating that the interaction between CBP and PME3 is highly specific (see Supplemental Figure 5B online).

To identify the region of amino acids of CBP required for the interaction with PME3, a series of deletions of the *CBP* sequence in the bait vector was generated and the interaction was examined by α-Gal quantitative assay after cotransformation of bait and prey plasmids into the requisite yeast strain. N-terminal Hs CBP amino acid deletions Δ1-72 and Δ1-97 showed only weak interaction with PME3 (Figure 2C). However, the shorter N-terminal amino acid deletion Δ1-47 gave rise to an increased interaction when compared with the complete CBP sequence. This finding indicates that the first 47 amino acids of CBP are not critical for the interaction and that the next 25 amino acids are necessary for binding to PME3. To test this possibility, a bait plasmid containing only amino acids 48 to 88 was generated. This bait construct was found to bind to the prey and gave rise to strong α-Gal activity. Finally, a bait construct containing only amino acids 48 through 72 gave rise to the strongest interaction (Figure 2C), indicating that these 25 amino acid residues are necessary and sufficient for recognition and binding of PME3 in the Y2H system.

Subcellular Localization of PME3 and Temporal Expression during *H. schachtii* Infection

To investigate the subcellular localization of PME3, the 3′-end of the *PME3* coding sequence (with or without the native signal peptide coding region) was cloned before the start codon of a joined GFP-GUS coding sequence construct, thus giving rise to a *PME3*:GFP:GUS translational fusion protein that is big enough to prevent passive diffusion among cell compartments. This gene construct was expressed in onion epidermal cells. After plasmolysis, the GFP signal was detected only in the cytoplasm of the onion cells bombarded with the fusion construct containing *PME3* without the signal peptide. However, when the *PME3* construct with signal peptide was fused to GFP, the reporter protein was detected both in the cell wall and the cytoplasm (Figure 3A). These results corroborate our Y2H-predicted CBP-PME3 in planta interaction since both proteins can be found within the plant cell cytoplasm.

If indeed PME3 has a function during cyst nematode parasitism, it is conceivable that *PME3* mRNA abundance may change during cyst nematode infection, potentially as a result of the

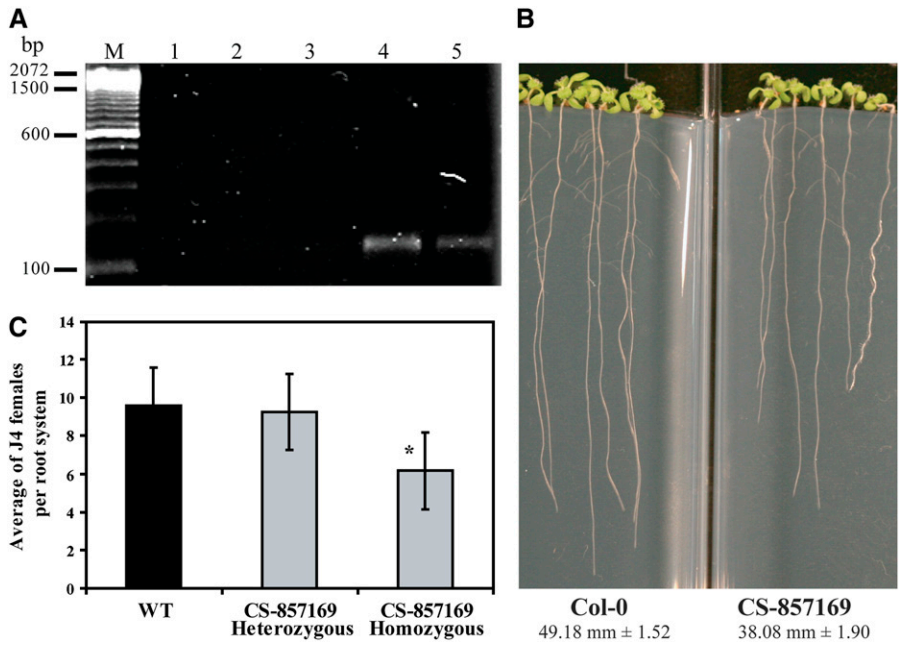

Figure 4. The *pme3* Knockout Mutant Is Altered in Root Length and Susceptibility to *H. schachtii*.

(A) *PME3* mRNA accumulation in the *pme3* mutant. *PME3* mRNA level was determined by quantitative real-time RT-PCR using gene-specific primers. The real-time RT-PCR products were resolved on syber safe-stained 2% agarose gel. No PCR products were detected after 40 cycles of amplification of cDNA from homozygous mutant plants (lanes 1 to 3), whereas specific amplifications were detected after amplification of cDNA from either heterozygous (lane 4) or wild-type (Col-0) plants (lane 5). Molecular weight marker is a 100 bp ladder (Invitrogen).

(B) The *pme3* knockout mutant develops shorter roots than the wild-type (Col-0). Homozygous plants were planted on modified Knop's medium with the wild type (Col-0), and root lengths were measured 15 d after planting. Root length values are averages of at least 30 plants ± SE. Differences between *pme3* and the wild type were statistically significant as determined by unadjusted paired *t* tests ($P < 0.01$).

(C) The *pme3* knockout mutant is less susceptible to *H. schachtii* than the wild type (Col-0). The *pme3* knockout mutant (homozygous and heterozygous) and wild-type (Col-0) plants were planted on modified Knop's medium, and 2-week-old seedlings were inoculated with ~250 surface-sterilized J2 *H. schachtii*. Two weeks after inoculation, the number of J4 female nematodes per root system was counted. Data are presented as the mean ± SE. Mean values significantly different from that of the wild type as determined by unadjusted paired *t* tests ($P < 0.05$) are denoted by an asterisk. Identical results were obtained from at least four independent experiments.

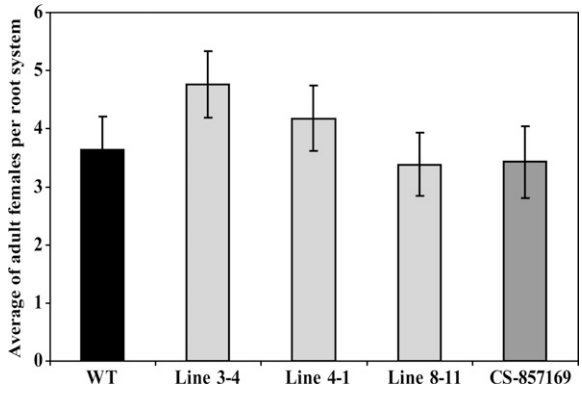

Figure 5. Root-Knot Nematode Susceptibility Is Not Altered in *PME3*-Overexpressing Lines and the *pme3* Knockout Mutant.

Homozygous T3 lines overexpressing *PME3* (lines 3-4, 4-1, and 8-11) or the *pme3* knockout mutant (CS-857169) as well as wild-type (Col-0) plants were planted on modified Knop's medium, and 2-week-old seedlings were inoculated with ~250 surface-sterilized J2 *M. incognita*. Four weeks after inoculation, the numbers of adult egg-laying female nematodes per root system were counted. No statistically significant differences between the tested lines and the wild-type control were detected. Data are presented as the mean ± SE. Identical results were obtained from two independent experiments.

protein–protein interaction or other mechanisms. *PME3* mRNA was quantified in triplicate quantitative real-time RT-PCR assays using gene-specific primers designed to discriminate between different members of the PME gene family (see Methods). Two-week-old wild-type *Arabidopsis* seedlings were inoculated with *H. schachtii*, and root and shoot tissues were harvested from treated and control plants at 3, 8, and 14 d post inoculation for RNA extraction. Data from three independent experiments revealed that *PME3* mRNA was upregulated in *H. schachtii*–inoculated roots at all time points when compared with noninfected roots. The strongest induction was observed at the 8-d time point (Figure 3B). Interestingly, *PME3* mRNA abundance was much weaker in shoots than in roots, and significant upregulation was only seen at the 8-d time point (Figure 3B). Quantifying the gene expression level of *PME3* in root versus shoot tissues of 2- to 3-week-old uninfected *Arabidopsis* plants revealed a >58-fold higher *PME3* expression in roots when compared with shoots.

PME3 Expression Levels Correlate with *Arabidopsis* Susceptibility

To provide additional information about the involvement of PME3 in the plant response to *H. schachtii*, transgenic *Arabidopsis* lines overexpressing the full-length *PME3* cDNA with the signal peptide and under the control of 35S CaMV promoter were generated and phenotypically investigated. Independent T3 homozygous lines developed longer roots and taller shoots than Col-0 wild-type plants (Figures 3C and 3D). When transgenic lines were assayed for nematode susceptibility, all three T3 homozygous lines tested (3-4, 4-1, and 8-11) supported significantly higher numbers of adult females than wild-type plants (Figure 3E). These findings indicate that, much like CBP, PME3 activity is conducive to *H. schachtii* parasitism.

To further explore *PME3* function, we screened a T-DNA insertion mutant database at The Arabidopsis Information Resource (Alonso et al., 2003) and identified a T-DNA–tagged *PME3* insertional mutant (CS857169). Sequence analysis of this mutant allele revealed that the T-DNA insertion is located in the likely promoter at 305 nucleotides upstream of the start codon. Quantitative real-time RT-PCR analysis of *PME3* mRNA abundance in homozygous mutant plants using gene-specific primers failed to detect any transcript even after high numbers of PCR amplification cycles. By contrast, specific amplifications were detected in both heterozygous and wild-type plants (Figure 4A). To address whether the knockout mutation of *PME3* affected root length, because we observed larger roots in overexpression lines, we examined 15-d-old seedlings grown on nutrient medium. We determined that the root length of mutant plants was significantly shorter (38.08 mm ± 1.90 mm) than that of the wild type (49.18 mm ± 1.52 mm) (Figure 4B), which is in line with the overexpression phenotype described above. Most importantly, we also determined the susceptibility to *H. schachtii* of *pme3* knockout mutants in three independent experiments. Compared with the wild type, mutant plants were significantly less susceptible to *H. schachtii* (Figure 4C).

As was performed for *CBP*-expressing *Arabidopsis* lines, we assayed *PME3*-overexpressing lines and the knockout mutant for susceptibility to *M. incognita*. These assays did not reveal altered susceptibility phenotypes of these lines (Figure 5), documenting that the PME3 effects, much like CBP, are specific for the cyst nematode interaction.

To provide additional evidence for the direct connection between CBP and PME3, we measured PME activity in the transgenic plants expressing CBP (line 2-4), the *pme3* knockout mutant, and the *PME3* overexpression plants (line 3-4) under noninfected conditions. As expected, the *pme* knockout mutant showed an ~15% decrease in PME activity, while PME3 overexpression plants exhibited a dramatic increase of PME activity of almost 260% (Table 1). Interestingly, a small but statistically significant increase of PME activity of ~8% was detected in the

Table 1. PME Activity in Transgenic Plants Overexpressing Hs *CBP* or *PME3* and in the *pme3* Knockout Mutant

Line	PME Activity (nmol H^+/min/mg protein)	%	P Value
C24	341.3 ± 3.6	100	
CBP overexpressing line (2-4)	367.7 ± 3.9	108	0.01900
Col-0	371.8 ± 1.9	100	
pme3 knockout mutant	317.1 ± 6.0	85	0.04900
PME3 overexpressing line (3-4)	964.0 ± 7.6	259	0.00001

PME activity was measured in roots of 5-d-old plants. Data are presented as the mean ± SE. Mean values significantly different from the wild-type controls were determined by paired *t* tests ($P < 0.05$).

CBP-expressing plants compared with the wild-type control (Table 1). These findings support our finding of an effect of CBP on PME function and suggest that CBP interaction with PME3 increases this protein's activity.

Expression of *CBP* in the *pme3* Knockout Mutant

To determine whether CBP affects plant phenotypes exclusively through its interaction with PME3, we expressed *CBP* in the *pme3* knockout mutant, and four nonsegregating T2 lines were phenotypically analyzed. Interestingly, these transgenic plants showed significantly increased root lengths ranging from 43.72 mm ± 1.03 mm to 48.94 mm ± 1.09 mm compared with the *pme3* knockout mutant (35.23 mm ± 0.96 mm) (Figure 6A). However, the average increase of 32% was dramatically less than the 64% observed in wild-type plants expressing *CBP*. When these lines were used in nematode assays to determine plant susceptibility to *H. schachtii*, we observed a trend of weakly increased plant susceptibility compared with *pme3* knockout mutant. However, these changes were statistically not significant (Figure 6B). These data indicate that CBP in fact requires PME3 for the majority of the observed phenotypic effects but that other, minor mechanisms also do exist.

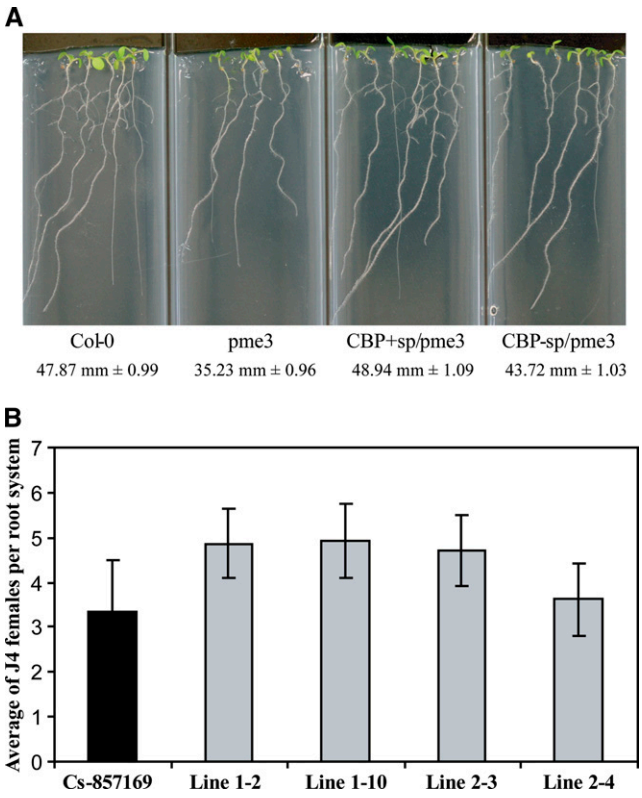

Figure 6. Overexpression of *CBP* in the *pme3* Knockout Mutant.

pme3 knockout mutant plants expressing *CBP* with or without signal peptide exhibited significantly longer root systems when compared with the *pme3* knockout mutant at 14 d after planting **(A)** and nonsignificant increases of *H. schachtii* susceptibility **(B)** as determined by unadjusted paired *t* tests ($P < 0.05$). Root length values are averages of at least 30 plants ± SE.

DISCUSSION

Identification of both nematode and host proteins involved in key processes of the compatible plant–nematode interaction will provide insights into the mechanisms of successful parasitism. At the same time, these studies reveal valuable insights into general plant biology as new functions of plant proteins are discovered. The soybean cyst nematode has been shown to produce a unique secretory CBP consisting only of a CBD without a catalytic domain (Gao et al., 2004). Several lines of evidence suggest that CBP is secreted during parasitism. First of all, there is no cellulose within the nematode and CBP genes are not found in any nonparasitic or animal-parasitic nematodes, indicating that the site of action is within the plant tissue. Furthermore, the presence of an N-terminal signal peptide and the absence of transmembrane domain motifs in the protein sequence, together with the CBP gene's exclusive expression in the nematode secretory subventral gland cells, document that CBP is a secreted protein involved in parasitism. If indeed CBP has the important function in pathogenesis as hypothesized, its gene should be expressed during a defined period of parasitic stages. Indeed, we observed high increases of *CBP* mRNA abundance in the parasitic J2 and an expression peak in the J3 stages, which suggests a role in parasitism during the time period after penetration into the plant root and particularly during early syncytium formation and development. In this period, cell walls are dramatically altered/remodeled during nematode migration as well as during extensive incorporation of root cells into the syncytium. The ability of the recombinant Hg CBP protein to bind to cellulose in in vitro assays (Gao et al., 2004) again supports a role of CBP inside plant tissues where cellulose represents an ubiquitous molecule. Finally, detection of a CBP in stylet secretions of *M. incognita* J2 (Ding et al., 1998) provides strong evidence that CBPs are secreted proteins with functions in plant tissues during nematode parasitism.

Expressing parasitism genes in plant hosts to assess their effects on plant phenotype and nematode susceptibility provides a meaningful way to functionally characterize parasitism proteins (Wang et al., 2005; Huang et al., 2006). We expressed the Hs *CBP* cDNA in *Arabidopsis*, which resulted in increased root length compared with wild-type controls. This observation is in agreement with the previously reported functional role of bacterial CBDs in living plant cells. Shpigel et al. (1998) reported that the CBD of the CBP of *C. cellulovorans* enhanced elongation of peach pollen tubes and *Arabidopsis* roots when it was exogenously applied at low concentrations. Recently, transgenic potato plants producing a bacterial CBP were found to be taller and larger than wild-type plants at early stages of development but did not differ significantly at later developmental stages (Safra-Dassa et al., 2006), suggesting that this CBP can function in a stage-dependent manner, potentially correlated with elevated rates of cell division.

The fact that CBP serves an important function during the plant–nematode interaction became evident through the significantly elevated susceptibility of *Arabidopsis* plants expressing Hs *CBP*. This result was further confirmed by our finding that the increased root size per se was not the cause of the increase in the number of nematodes penetrating into the roots but that rather a

cyst nematode-specific root alteration had taken place that allowed higher parasitic success postpenetration. These data along with our expression analyses indicate that CBP most likely functions not during the penetration phase of infection but rather during early phases of syncytium formation. Interestingly, our data revealed no significant difference in syncytia size between the transgenic *CBP*-expressing lines and wild-type plants. The functional role of CBP in facilitating nematode parasitism, therefore, could be accelerated feeding site development.

Like *CBP*, *PME3* showed convincing cause to postulate an important role during parasitism. *PME3* overexpression lines showed phenotypes similar to *CBP* overexpression, including a significantly elevated susceptibility to cyst nematodes. By contrast, knocking out *PME3* resulted in the exact opposite phenotypes of shorter roots and reduced susceptibility. PME3, therefore, plays a crucial role in cyst nematode parasitism, which also gives additional credence to the conclusion that the interaction with PME3 is of importance for the function of CBP. In addition, the soybean ortholog of *PME3* (BE821923) was shown to be upregulated within the actual developing syncytia induced by the soybean cyst nematode *H. glycines* (Ithal et al., 2007), which provides additional evidence of a role for PME3 in the cyst nematode infection process. Most importantly, a direct functional connection between PME3 and *CBP* is supported by our finding that transgenic plants expressing Hs CBP exhibited higher PME activity than wild-type controls. The observed 8% increase in PME activity is even more impressive when considering that (1) the employed assay measures all root PME activity, consisting of numerous enzymes and that CBP appears to only interact with PME3; and (2) mutational knockout of *PME3* resulted in an activity loss of only 15%. Furthermore, the root preferential expression of *PME3* most likely is the cause of the root-specific phenotypes in *CBP*-expressing *Arabidopsis* lines and again highlights the relevance of the interaction between both proteins.

Several pieces of evidence have indicated that PMEs contribute to cell growth by regulating the mechanical and chemical properties of plant cell walls via demethylesterification of pectin (Micheli, 2001). Transgenic potato plants overexpressing pectin methylesterase were characterized by relatively rapid elongation at early stages of development (Pilling et al., 2000). The enlarged size of plants overexpressing CBP or PME3 may be attributable to this type of PME action. It has been suggested that PMEs also have a role in resistance to fungal and bacterial pathogens (McMillan et al., 1993; Boudart et al., 1998; Wietholter et al., 2003) by affecting the physicochemical properties of the cell wall to be more accessible to cell wall–digesting enzymes (Lionetti et al., 2007). Interestingly, we did not find significant effects of CBP or PME3 on plant susceptibility to *M. incognita*. The finding that CBP and PME are specific to cyst nematodes can be explained by the fact that CBP functions during syncytium formation and the fact that root-knot nematodes induce completely different feeding sites, termed giant cells, that are derived through unrelated etiology despite the relatively close phylogenetic relationship between both nematodes.

Due to the new insights provided here, the mechanism by which CBP facilitates nematode parasitism becomes clearer. Taken together, our results show that this parasitism protein functions during syncytium formation through its interaction with PME3. However, it remains unclear where these two proteins interact. Despite our findings that CBP, when produced in planta, is most probably a cytoplasm-localized protein, it appears likely that, ultimately, CBP functions in the cell wall, given the fact that the cell wall is the site of cellulose accumulation and also where PME3 is expected to be localized. In this scenario, CBP would be secreted by the nematode using its stylet into the host plant cytoplasm from where it is hypothesized to be exported into the apoplast and the cell wall. Because we observed PME3 in the cytoplasm as well as the cell wall, interaction with CBP could be in the cytoplasm followed by a potential joint export. Ultimately, further research has to address this remaining question.

Our data further suggest that CBP functions in the targeting (to cellulose-associated pectin) and/or activation of PME3 to reduce the level of methylesterification of pectin in the cell wall. The opposite relationship between PME activity and pectin methylesterification level has been described in the literature (Lionetti et al., 2007). Therefore, it appears most likely that a reduction of cell wall pectin methylesterification through CBP-mediated increased and targeted PME3 activity allows improved access of other cell wall–modifying enzymes to cell wall polymers, thereby accelerating enzymatic activities, which is a requirement for syncytium development. In support, the ability of polygalacturonases and pectate lyases to degrade the pectin main chain has been shown to depend on the activity of PME (Christgau et al., 1996). By contrast, the expected high level of methylesterified pectin in the *pme3* knockout mutant would hamper the activity of cell wall–modifying enzymes and consequently reduce their effectiveness resulting in reduced susceptibility, which is what we observed in the nematode susceptibility assays. Expression of *CBP* in the *pme3* knockout mutant resulted in a slight increase of nematode susceptibility of ~34% compared with the *pme3* mutant. However, this percentage is much lower than the 78% observed when CBP was expressed in the wild type, showing that the CBP–PME3 interaction is a required, but not the sole, mechanism for the increased susceptibility observed in *CBP*-overexpressing lines. Similarly, *CBP* expression in the *pme3* knockout mutant resulted in only a 32% increase of root length compared with the 64% increase when *CBP* was expressed in the wild type. This is an example of a molecular plant–animal interaction using a bipartite cooperative means of cell wall modification to further the parasitic success of the nematode. In conclusion, reducing the level of methylesterified pectin in the cell walls of presyncytial cells during the early stages of syncytium formation through the activation/targeting of PME3 is the most likely mode of action of CBP in facilitating parasitism.

METHODS

Plant Materials and Growth Conditions

Arabidopsis thaliana seeds were surface-sterilized in 50% bleach for 5 min followed by four rinses in sterile water. Plants were grown under sterile conditions on Murashige and Skoog (MS) medium (PlantMedia) containing 2% sucrose solidified with 0.8% phyto agar (RPI) or in Metro-Mix 200 soil mixture (Sun Gro Horticulture) in a growth chamber (16 h light/8 h dark) at 23°C. *Arabidopsis* ecotype C24 was used as the wild type

for overexpression of Hs CBP, while ecotype Columbia-0 (Col-0) was used for overexpression of PME3. For phenotypic assays of overexpressing lines or knockout mutant lines, the corresponding wild type was used for comparison.

Plasmid Construction and Generation of Transgenic *Arabidopsis* Plants

The coding sequences of Hs *CBP* with or without the nematode signal peptide (SP) sequence were amplified from the full-length cDNA clone (EU328302) with primers CBP(SP) forward (5′-TATAGGATCCATGAATTGGATGCATTATTGTTTAATC-3′) or CBP forward (5′-TATAGGATCCATGTCCACTATTAATTCGGTAACCGTAC-3′) and CBP reverse (5′-ATGATGAGCTCTAGGGCAATTAGCTTAATTGGGTAGG-3′), which contained *Bam*HI or *Sac*I restriction sites (underlined) for directional cloning. PCR amplification was performed using the Expand High Fidelity^{plus} PCR system (Roche) according to the manufacturer's instructions. PCR products were digested by *Bam*HI and *Sac*I, gel purified, and ligated into the binary vector pBI121. Cloned products were verified by sequencing. The coding region of PME3 was amplified from *Arabidopsis* cDNA as described above using gene-specific primers designed to create the *Xba*I and *Xho*I restriction sites in the forward and reverse primers, respectively. The primer sequences used were PME forward 5′-CTCTAGAATGGCACCATCAATGAAAGAAATT-3′ and PME reverse 5′-CCTCGAGTCAAAGACCGAGCGAGAAGGG-3′ (restriction sites are underlined). The amplified products were digested by *Xba*I and *Xho*I, gel purified, ligated into *Xba*I-*Xho*I restriction sites of the binary vector pBI121, transformed, and confirmed by sequencing. *Agrobacterium tumefaciens* strain C58 was transformed with the binary plasmids by the freeze-thaw method (An et al., 1988) and used to transform *Arabidopsis* wild-type C24, Col-0, or *pme3* knockout mutant plants as described by Clough and Bent (1998). Transformed T1 plants were screened on MS medium containing 50 mg/L kanamycin to select for transgenic plants. Homozygous T3 seeds were collected from T2 lines after segregation analysis on kanamycin-containing medium.

Root Length Measurements

Seeds were surface sterilized and transferred to Nunc 4 well Polystyrene Rectangular Dishes (Thermo Fisher Scientific) containing MS medium. Plates were incubated in a vertical position in a growth chamber at 23°C under 16-h-light/8-h-dark conditions. At the time of measurement, the root length of at least 10 plants per treatment was measured as the distance between the crown and the tip of the main root in three independent experiments. Statistically significant differences between lines were determined by unadjusted paired *t* test ($P < 0.01$).

Nematode Infection Assay

Transgenic *Arabidopsis* seeds (T3 generation) and wild-type controls (Col-0 and C24) were surface sterilized and planted in a random block design in 12-well Falcon culture plates (BD Biosciences) containing modified Knop's medium (Sijmons et al., 1991) solidified with 0.8% Daishin agar (Brunschwig Chemie). Plants were grown at 24°C under 16-h-light/8-h-dark conditions. Two-week-old seedlings were inoculated with ~250 surface-sterilized J2 *Heterodera schachtii* or *Meloidogyne incognita* nematodes as previously described by Baum et al. (2000). Inoculated plants were maintained under the conditions described above for an additional 2 weeks before the number of *H. schachtii* J4 females were counted. In the case of *M. incognita*, the number of J4 females was counted 4 weeks after inoculation.

Nematode Penetration Assay

The penetration rate of *H. schachtii* second-stage juveniles was studied in lines 21-9 and BV2-26-3 and compared with wild-type *Arabidopsis* C24. The three lines were planted in a random-block design on modified Knop's medium in 12-well culture plates as described above. At 10 d, each plant was inoculated with 150 surface-sterilized J2 of *H. schachtii*, and the plates placed back in the incubator for 4 additional days. Then, each well was stained for the presence of penetrating nematodes using a modified version of the protocol from Grundler et al. (1991). In short, nematodes were stained by adding 1 mL of fixation/staining solution (500 mL acetic acid, 500 mL 96% ethanol, and 17 mg acid fuchsin) and incubated at room temperature for 24 h. Each well was then rinsed with water, and 1 mL of destaining solution (600 mL water, 200 mL glycerine, and 200 mL lactic acid) was added. The number of penetrating nematodes in each root system was counted by observing the root systems under bright-field illumination at ×200 using a Zeiss Axiovert 100 microscope. Each plant line was replicated 18 times, and two independent experiments were conducted. Average numbers of penetrating nematodes were calculated, and statistically significant differences were determined in a modified *t* test using the statistical software package SAS.

Syncytial Measurements

Syncytial measurements were taken 24 d after inoculation of *H. schachtii* onto the three subject lines. For each line, 10 single-female syncytia were randomly selected and photographed on a Zeiss Stemi SV11 dissecting microscope using a Zeiss AxioCam MRc5 digital camera. The digital files were then processed using Zeiss Axiovision software (release 4.4). For each photographed syncytium, the image was processed with the Axiovision measure tool and calibrated against the correct scaling of the original image from the Stemi SV11. The measurements were aided by the use of a Wacom Intuos 3 9x12 drawing tablet (Wacom Technology). Using the tablet, the syncytial cells were outlined, and total area for the syncytium was calculated as square millimeters. The individual measurements for the syncytium of each line were used to calculate an average syncytial size for each line tested using the statistical software package SAS. Significance of size differences between lines was determined via a modified *t* test in SAS ($P < 0.05$).

RNA Isolation and Quantitative Real-Time RT-PCR

Total RNA was extracted from 100 mg frozen ground plant tissues using the RNeasy plant mini kit (Qiagen) or from 50 mg nematode tissues using the Versagene RNA tissue kit (Gentra Systems) following the manufacturer's instructions. DNase treatment of total RNA was performed using DNase I (Invitrogen). Gene-specific primers to Hs *CBP*, *PME3*, *H. schachtii actin* (AY443352), and *Arabidopsis actin* (AT1G49240) were designed. For real-time RT-PCR in *H. schachtii*, 10 ng of DNase-treated RNA were used for cDNA synthesis and PCR amplification using the one-step RT-PCR kit (Bio-Rad) according to the manufacturer's protocol. The PCR reactions were run in an I Cycler (Bio-Rad) using the following program: 50°C for 10 min, 95°C for 5 min, and 40 cycles of 95°C for 30 s and 60°C for 30 s. Following PCR amplification, the reactions were subjected to a temperature ramp to create the dissociation curve, determined as changes in fluorescence measurements as a function of temperature, by which the nonspecific products can be detected. The dissociation program was 95°C for 1 min, 55°C for 10 s, followed by a slow ramp from 55°C to 95°C. For real-time RT-PCR in *Arabidopsis*, first-strand cDNA was synthesized from DNase-treated RNA using the Advantage RT-for-PCR kit (Clontech) according to the manufacturer's instructions. The synthesized cDNAs then were diluted to a concentration equivalent to 10 ng total RNA/μL and used as a template in real-time RT-PCR reactions using the two-step RT-PCR kit (Bio-Rad) according to manufacturer's protocol. In all cases, at least three independent experiments each with three technical replicates of each reaction were performed. *Arabidopsis* and nematode *actin*, as constitutively expressed genes,

were used as internal controls to normalize gene expression levels. Quantification of the relative changes in gene expression was performed using the $2^{-\Delta\Delta CT}$ method as described by Livak and Schmittgen (2001).

Subcellular Localization

The Hs *CBP* and *PME3* coding sequences with and without signal peptide-encoding regions were amplified using gene-specific primer pairs containing *Hin*dIII and *Xba*I restriction enzyme sites in the forward and reverse primers, respectively. For CBP, the primer sequences used were CBP(SP) forward (5′-TATAAAGCTTATGAATTGGATGCATT-ATTGTTTAATC-3′) or CBP forward (5′-TATAAAGCTTATGTCCACTAT-TAATTCGGTAACCGTAC-3′) and CBP reverse (5′-ATGATTCTAGATTT-TTTTGCATTGTTTGCTGGTTGGA-3′). For *PME3*, primer sequences used were PME3(SP) forward (5′-TATAAAGCTTATGGCACCATCAATGAAA-GAAATTTTTTC-3′) or PME3 forward (5′-TATAAAGCTTATGATCTCTG-CCGGAGCTTCAAAAGCC-3′) and PME3 reverse (5′-ATGATTCTAGA-TAAGACCGAGCGAGAAGGGGAAACCG-3′). The resulting amplified fragments were cloned into the respective sites in the modified pRJG23 vector (Grebenok et al., 1997) before the start codon of GFP fused into the GUS reporter gene and under the control of double CaMV 35S promoter. All constructs were confirmed by DNA sequencing. These constructs were delivered into onion epidermal cells by biolistic bombardment as described by Elling et al. (2007b). After bombardment, epidermal peels were incubated for 24 h in the dark. Plasmolysis of onion epidermal cells was achieved by soaking the cells in 1 M sucrose solution for 15 min. The subcellular localization of the fused proteins was visualized using a Zeiss Axiovert 100 microscope. The transient transformation experiments were repeated at least three times independently.

Y2H Assays

A Y2H screening was performed as described in the BD Matchmaker Library Construction and Screening Kits (Clontech). The complete coding sequence of CBP was fused to the GAL4 DNA binding domain (BD) of pGBKT7 to generate pGBKT7-CBP and then introduced into *Saccharomyces cerevisiae* strain Y187 to generate the bait strain. Three *Arabidopsis* cDNA libraries from roots of ecotype C24 at 3, 7, and 10 d after *H. schachtii* infection were generated in *S. cerevisiae* strain AH109, as fusion to the GAL4 activation domain (AD) of pGADT7-Rec2 vector. Screening for interacting proteins and subsequent analyses were performed as described in Clontech protocols.

BiFC Analysis of Hs CBP and PME3

The *CBP* cDNA without signal peptide was PCR-amplified using forward primer (5′-TATAGAATTCATCCACTATTAATTCGGTAACCGTAC-3′) and reverse primer (5′-ATGATTCTAGATCATTTTTTGCATTGTTTGCT-GGTTGGA-3′) containing *Eco*RI and *Xba*I restriction sites (underlined), respectively, and cloned into *Eco*RI-*Xba*I sites of pSAT4-nEYFP-C1 to generate pSAT4-nEYFP-CBP. Meanwhile, the full-length *PME3* cDNA without signal peptide was PCR amplified using forward primer (5′-TATAGAATTCAATCTCTGCCGGAGCTTCAAAAGCC-3′) and reverse primer (5′-ATGATTCTAGATCAAAGACCGAGCGAGAAGGGGAAA-CCG-3′) containing *Eco*RI and *Xba*I restriction sites (underlined), respectively, and cloned into *Eco*RI-*Xba*I sites of pSAT4-cEYFP-C1(B) to generate pSAT4-cEYFP-PME3. Both plasmids were confirmed by sequencing. For coexpression, particle bombardment was performed using onion epidermal cells. Gold particles (1.6 μm diameter) (Bio-Rad) were washed with 100% ethanol and coated with 1.5 μg of each DNA using standard procedures. cDNA-coated gold particles were bombarded at 1100 p.s.i. and 9 cm distance using a Biolistic Particle Delivery System PDS-1000/He (Bio-Rad). Bombarded tissues were incubated at 25°C in darkness for ~24 h before being assayed for YFP activity. The bright-field and fluorescent images were taken using the Zeiss Axiovert 100 microscope with appropriate YFP filter.

PME Activity

The PME-containing protein fractions were extracted from root tissues using a high-salt buffer as described by Ren and Kermode (2000). The root tissues of 5-d-old *Arabidopsis* plants were collected and fully ground in liquid nitrogen and then homogenized with 200 μL PME extraction buffer (0.1 M citrate acid, 0.2 M Na_2HPO_4, and 1 M NaCl, pH 5.0). The homogenized materials were incubated on ice for 1 h, during which they were mixed three times at 20-min intervals, and finally centrifuged for 10 min at 14,000 rpm at 4°C. The supernatant was collected and the crude protein content was quantified using a Pierce BCA-200 protein assay kit (Pierce) following the manufacturer's instructions. PME activity was assayed according to the method described by Richard et al. (1994). Two micrograms of protein samples were added to 4 mL of substrate solution containing 0.5% citrus pectin (Sigma-Aldrich), 0.2 M NaCl, and 0.002% methyl red, pH 6.8, for 1 h at 37°C. Pectin de-esterification decreases the pH, thus changing the color from yellow to red. The color change was measured using a spectrophotometer (UV-Vis Spectrophotometer; Cary 50 Bio) as OD at 525 nm. A calibration curve was obtained by adding 5 to 30 μL 0.01 M HCl to 4 mL of substrate solution and measuring the respective OD values at 525 nm. PME activity of different samples (nmol H^+/min/mg protein) was obtained according to the calibration curve.

In Situ Hybridization

Specific forward and reverse primers for the Hs *CBP* cDNA clone were used to synthesize a digoxigenin (DIG)-labeled sense and antisense cDNA probes (Roche) by PCR. In situ hybridizations were performed using mixed parasitic stages of *H. schachtii* as described by de Boer et al. (1998). Hybridization signals within the nematodes were detected with alkaline phosphatase-conjugated anti-DIG antibody and substrate, and specimens were observed with a Zeiss Axiovert 100 inverted light microscope.

Accession Numbers

Sequence data from this article can be found in the Arabidopsis Genome Initiative or GenBank/EMBL databases under the following accession numbers: *Arabidopsis actin* (AT1G49240), *H. schachtii actin* (AY443352), Hg CBP (AY340946), Hs CBP (EU328302), *PME1* (At1g53840), *PME2* (At1g53830), and *PME3* (At3g14310). The Arabidopsis Information Resource stock number for *PME3* insertional mutant is CS857169.

Supplemental Data

The following materials are available in the online version of this article.

Supplemental Figure 1. Sequence Alignment of Hg CBP and Hs CBP.

Supplemental Figure 2. In Situ Hybridization and Developmental Expression Level of Hs *CBP*

Supplemental Figure 3. Hs *CBP* Expression in *Arabidopsis* Does Not Alter Nematode Penetration into Roots.

Supplemental Figure 4. Hs *CBP* Expression in *Arabidopsis* Does Not Alter Susceptibility to the Root-Knot Nematode.

Supplemental Figure 5. Hs CBP Specifically Interacts with PME3.

Supplemental Table 1. Quantification of Hs *CBP* Expression Levels in Transgenic *Arabidopsis* Lines Using Quantitative Real-Time RT-PCR.

ACKNOWLEDGMENTS

This is a journal paper of the Iowa Agriculture and Home Economics Station, Ames, IA, supported by Hatch Act and State of Iowa funds. This work was funded by USDA National Research Initiative Competitive Grants Program Award 2005-35604-15434 and by grants from the Iowa Soybean Association. We thank Stanton Gelvin for providing the BiFC vectors and Calvin Tan for technical assistance.

Received September 4, 2008; revised October 15, 2008; accepted October 29, 2008; published November 11, 2008.

REFERENCES

Alonso, J.M., et al. (2003). Genome-wide insertional mutagenesis of *Arabidopsis thaliana*. Science **301:** 653–657.

An, G., Ebert, P.R., Mitra, A., and Ha, S.B. (1988). Binary vectors. In Plant Molecular Biology Manual, S.B. Gelvin, R.A. Schilperoort, and D.P.S. Verma, eds (Dordrecht, The Netherlands: Kluwer Academic Publishers), 1–19.

Barker, K.R., and Koenning, S.R. (1998). Development of sustainable systems for nematode management. Annu. Rev. Phytopathol. **36:** 165–205.

Baum, T.J., Wubben II, M.J.E., Hardy, K.A., Su, H., and Rodermel, S.R. (2000). A screen for *Arabidopsis thaliana* mutants with altered susceptibility to *Heterodera schachtii.* J. Nematol. **32:** 166–173.

Boudart, G., Lafitte, C., Barthe, J.P., Frasez, D., and Esquerré-Tugayé, M.T. (1998). Differential elicitation of defense responses by pectic fragments in bean seedlings. Planta **206:** 86–94.

Carrard, G., Koivula, A., Söderlund, H., and Béguin, P. (2000). Cellulose-binding domains promote hydrolysis of different sites on crystalline cellulose. Proc. Natl. Acad. Sci. USA **97:** 10342–10347.

Christgau, S., Kofod, L.V., Halkier, T., Anderson, L.N., Hockauf, M., Dorreich, K., Dalboge, H., and Kauppinen, S. (1996). Pectin methyl esterase from *Aspergillus aculeatus*: Expression cloning in yeast and characterization of the recombinant enzyme. Biochem. J. **319:** 705–712.

Clough, S.J., and Bent, A.F. (1998). Floral dip: A simplified method for Agrobacterium-mediated transformation of *Arabidopsis thaliana.* Plant J. **16:** 735–743.

Collmer, A., and Keen, N.T. (1986). The role of pectic enzymes in plant pathogenesis. Annu. Rev. Phytopathol. **24:** 383–409.

Davis, E.L., Hussey, R.S., and Baum, T.J. (2004). Getting to the roots of parasitism by nematodes. Trends Parasitol. **20:** 134–141.

Davis, E.L., Hussey, R.S., Mitchum, M.G., and Baum, T.J. (2008). Parasitism proteins in nematode-plant interactions. Curr. Opin. Plant Biol. **11:** 360–366.

de Boer, J.M., McDermott, J.P., Davis, E.L., Hussey, R.S., Popeijus, H., Smant, G., and Baum, T.J. (2002). Cloning of a putative pectate lyase gene expressed in the subventral esophageal glands of *Heterodera glycines.* J. Nematol. **34:** 9–11.

de Boer, J.M., Yan, Y., Bakker, J., Davis, E.L., and Baum, T.J. (1998). *In situ* hybridization to messenger RNA of *Heterodera glycines*. J. Nematol. **30:** 309–312.

de Boer, J.M., Yan, Y., Wang, X., Smant, G., Hussey, R.S., Davis, E.L., and Baum, T.J. (1999). Developmental expression of secretory β-1,4-endoglucanases in the subventral esophageal glands of *Heterodera glycines.* Mol. Plant Microbe Interact. **12:** 663–669.

Ding, X., Shields, J., Allen, R., and Hussey, R.S. (1998). A secretory cellulose-binding protein cDNA cloned from the root-knot nematode (*Meloidogyne incognita*). Mol. Plant Microbe Interact. **11:** 952–959.

Doi, R.H., and Kosugi, A. (2004). Cellulosomes: Plant-cell-wall-degrading enzyme complexes. Nat. Rev. Microbiol. **7:** 541–551.

Elling, A.A., Davis, E.L., Hussey, R.S., and Baum, T.J. (2007b). Active uptake of cyst nematode parasitism proteins into the plant cell nucleus. Int. J. Parasitol. **37:** 1269–1279.

Elling, A.A., et al. (2007a). Divergent evolution of arrested development in the dauer stage of Caenorhabditis elegans and the infective stage of *Heterodera glycines.* Genome Biol. **8:** R211.

Gao, B., Allen, R., Davis, E.L., Baum, T.J., and Hussey, R.S. (2004). Molecular characterization and developmental expression of a cellulose-binding protein gene in the soybean cyst nematode *Heterodera glycines.* Int. J. Parasitol. **34:** 1377–1383.

Gao, B., Allen, R., Maier, T., Davis, E.L., Baum, T.J., and Hussey, R.S. (2001). Identification of putative parasitism genes expressed in the esophageal gland cells of the soybean cyst nematode (*Heterodera glycines*). Mol. Plant Microbe Interact. **14:** 1247–1254.

Gao, B., Allen, R., Maier, T., Davis, E.L., Baum, T.J., and Hussey, R.S. (2003). The parasitome of the phytonematode *Heterodera glycines.* Mol. Plant Microbe Interact. **16:** 720–726.

Goellner, M., Smant, G., deBoer, J.M., Baum, T.J., and Davis, E.L. (2000). Isolation of beta-1,4-endoglucanase genes of *Globodera tabacum* and their expression during parasitism. J. Nematol. **32:** 154–165.

Goellner, M., Wang, X., and Davis, E.L. (2001). Endo-beta-1,4-endoglucanase expression in compatible plant nematode interactions. Plant Cell **13:** 2241–2255.

Goldstein, M.A., Takagi, M., Hashida, S., Shoseyov, O., Doi, R.H., and Segel, I.H. (1993). Characterization of the cellulose-binding domain of the *Clostridium cellulovorans* cellulose-binding protein A. J. Bacteriol. **175:** 5762–5768.

Grebenok, R.J., Pierson, E., Lambert, G.M., Gong, F.C., Afonso, C.L., Haldeman-Cahill, R., Carrington, J.C., and Galbraith, D.W. (1997). Green-fluorescent protein fusions for efficient characterization of nuclear targeting. Plant J. **11:** 573–586.

Grundler, F., Betka, M., and Wyss, U. (1991). Influence of changes in the nurse cell system (syncytium) on sex determination and development of the cyst nematode *Heterodera schachtii*: Total amounts of proteins and amino acids. Phytopath. **81:** 70–74.

Huang, G., Dong, R., Allen, R., Davis, E.L., Baum, T.J., and Hussey, R.S. (2006). A root-knot nematode secretory peptide functions as a ligand for a plant transcription factor. Mol. Plant Microbe Interact. **19:** 463–470.

Ithal, N., Recknor, J., Nettleton, D., Hearne, L., Maier, T., Baum, T.J., and Mitchum, M.G. (2007). Parallel genome-wide expression profiling of host and pathogen during soybean cyst nematode infection of soybean. Mol. Plant Microbe Interact. **20:** 293–305.

Lionetti, V., Raiola, A., Camardella, L., Giovane, A., Obel, N., Pauly, M., Favaron, F., Cervone, F., and Bellincampi, D. (2007). Overexpression of pectin methylesterase inhibitors in Arabidopsis restricts fungal infection by *Botrytis cinerea.* Plant Physiol. **143:** 1871–1880.

Livak, K.J., and Schmittgen, T.D. (2001). Analysis of relative gene expression data using real time quantitative PCR and the $2^{-\Delta\Delta CT}$ method. Methods **25:** 402–408.

McCartney, L., Blake, A.W., Flint, J., Bolam, D.N., Boraston, A.B., Gilbert, H.J., and Knox, J.P. (2006). Differential recognition of plant cell walls by microbial xylan-specific carbohydrate-binding modules. Proc. Natl. Acad. Sci. USA **103:** 4765–4770.

McMillan, G.P., Hedley, D., Fyffe, L., and Pérombelon, M.C.M. (1993). Potato resistance to soft-rot Erwinias is related to cell wall pectin esterification. Physiol. Mol. Plant Pathol. **42:** 279–289.

Micheli, F. (2001). Pectin methylesterases: Cell wall enzymes with important roles in plant physiology. Trends Plant Sci. **6:** 414–419.

Pilling, J., Willmitzer, L., and Fisahn, J. (2000). Expression of a *Petunia inflata* pectin methyl esterase in *Solanum tuberosum* L. enhances stem elongation and modifies cation distribution. Planta **210:** 391–399.

Qin, L., Kudla, U., Roze, E.H., Goverse, A., Popeijus, H., Nieuwland, J., Overmars, H., Jones, J.T., Schots, A., Smant, G., Bakker, J., and Helder, J. (2004). Plant degradation: A nematode expansin acting on plants. Nature **427:** 30.

Qin, L., Overmars, H., Helder, J., Popeijus, H., van der Voort, J.R., Groenink, W., van Koert, P., Schots, A., Bakker, J., and Smant, G. (2000). An efficient cDNA-AFLP-based strategy for the identification of putative pathogenicity factors from the potato cyst nematode *Globodera rostochiensis.* Mol. Plant Microbe Interact. **13:** 830–836.

Ren, C., and Kermode, A.R. (2000). An increase in pectin methyl esterase activity accompanies dormancy breakage and germination of yellow cedar seeds. Plant Physiol. **124:** 231–242.

Richard, L., Qin, L.X., Gadal, P., and Goldberg, R. (1994). Molecular cloning and characterization of a putative pectin methylesterase cDNA in *Arabidopsis thaliana* (L.). FEBS Lett. **355:** 135–139.

Safra-Dassa, L., Shani, Z., Danin, A., Roiz, L., Shoseyov, O., and Wolf, S. (2006). Growth modulation of transgenic potato plants by heterologous expression of bacterial carbohydrate-binding module. Mol. Breed. **17:** 355–364.

Shoseyov, O., and Doi, R.H. (1990). Essential 170-kDa subunit for degradation of crystalline cellulose by *Clostridium cellulovorans* cellulase. Proc. Natl. Acad. Sci. USA **87:** 2192–2195.

Shoseyov, O., Shani, Z., and Shpigel, E. (2001). Transgenic plants of altered morphology. US patent 6184440.

Shpigel, E., Roiz, L., Goren, R., and Shoseyov, O. (1998). Bacterial cellulose-binding domain modulates in vitro elongation of different plant cells. Plant Physiol. **117:** 1185–1194.

Sijmons, P.C., Grundler, F.M.W., Von Mende, N., Burrows, P.R., and Wyss, U. (1991). *Arabidopsis thaliana* as a new model host for plant parasitic nematodes. Plant J. **1:** 245–254.

Smant, G., et al. (1998). Endogenous cellulases in animals: Isolation of beta-1,4-endoglucanase genes from two species of plant-parasitic cyst nematodes. Proc. Natl. Acad. Sci. USA **95:** 4906–4911.

Tomme, P., Boraston, A., McLean, B., Kormos, J., Creagh, A.L., Sturch, K., Gilkes, N.R., Haynes, C.A., Warren, R.A., and Kilburn, D.G. (1998). Characterization and affinity applications of cellulose-binding domains. J. Chromatogr. B Analyt. Technol. Biomed. Life Sci. **715:** 283–296.

Wang, X., Meyers, D., Yan, Y., Baum, T., Smant, G., Hussey, R., and Davis, E. (1999). In planta localization of a β-1,4-endoglucanase secreted by *Heterodera glycines.* Mol. Plant Microbe Interact. **12:** 64–67.

Wang, X., Mitchum, M.G., Gao, B., Li, C., Diab, H., Baum, T.J., Hussey, R.S., and Davis, E.L. (2005). A parasitism gene from a plant-parasitic nematode with function similar to *CLAVATA3/ESR* (*CLE*) of *Arabidopsis thaliana.* Mol. Plant Pathol. **6:** 187–191.

Wang, X.H., Allen, R., Ding, X.F., Goellner, M., Maier, T., de Boer, J.M., Baum, T.J., Hussey, R.S., and Davis, E.L. (2001). Signal peptide-selection of cDNA cloned directly from the esophageal gland cells of the soybean cyst nematode *Heterodera glycines.* Mol. Plant Microbe Interact. **14:** 536–544.

Wietholter, N., Graessner, B., Mierau, M., Mort, A.J., and Moerschbacher, B.M. (2003). Differences in the methyl ester distribution of homogalacturonans from near-isogenic wheat lines resistant and susceptible to the wheat stem rust fungus. Mol. Plant Microbe Interact. **16:** 945–952.

Williamson, V.M., and Hussey, R.S. (1996). Nematode pathogenesis and resistance in plants. Plant Cell **8:** 1735–1745.

Wrather, J.A., Stienstra, W.C., and Koenning, S.R. (2001). Soybean disease loss estimates for the United States from 1996 to 1998. Can. J. Plant Pathol. **23:** 122–131.